Pupil dynamics for iris liveness detection

Adam Czajka, *Senior Member, IEEE*

***Abstract*—The primary objective of this paper is to propose a complete methodology for eye liveness detection based on pupil dynamics. This method may serve as a component of presentation attack detection in iris recognition systems, making them more secure. Due to a lack of public databases that would support this research, we have built our own iris capture device to register pupil size changes under visible light stimuli, and registered 204 observations for 26 subjects (52 different irides), each containing 750 iris images taken every 40 ms. Each measurement registers the spontaneous pupil oscillations and its reaction after a sudden increase of the intensity of visible light. The Kohn and Clynes pupil dynamics model is used to describe these changes; hence we convert each observation into a feature space defined by model parameters. To answer the question whether the eye is alive (that is, if it reacts to light changes as a human eye) or the presentation is suspicious (that is, if it reacts oddly or no reaction is observed), we use linear and non-linear Support Vector Machines to classify natural reaction and spontaneous oscillations, simultaneously investigating the goodness of fit to reject bad modeling. Our experiments show that this approach can achieve a perfect performance for the data we have collected: all normal reactions are correctly differentiated from spontaneous oscillations. We investigated the shortest observation time required to model the pupil reaction, and found that time periods not exceeding 3 seconds are adequate to offer a perfect performance.**

***Index Terms*—Liveness detection, pupil dynamics, iris recognition, presentation attack detection, biometrics.**

I. Introduction

FOR more than a decade liveness detection has been an important element of international discussion on biometric security. According to ISO/IEC, it concerns 'detection of anatomical characteristics or involuntary or voluntary reactions, in order to determine if a biometric sample is being captured from a living subject present at the point of capture' [1]. The ability to check the liveness is crucial to any biometric sensor. Even its name, *biometric*, is the synonym for dealing with living and authentic biological traits, and not with nonliving artifacts. Once the biometric sensor accepts artifacts or non-living body parts, the entire system deploying such sensor becomes moot.

Liveness detection refers to the detection of living symptoms, and hence is a special case of a wider class of techniques aiming at detection of any presentation attack. ISO/IEC defines the presentation attack as 'presentation of an artifact or human characteristic to the biometric capture subsystem in a fashion that could interfere with the intended policy of the biometric system'. This means that any subversive action (*i.e.*, with the *intention* to subvert a biometric system) should be detected as a presentation attack. However, the intention of the attacker cannot be inferred. Hence the presentation attack becomes a very broad-ranging field that includes presentation of fake objects, as well as cadaver parts, incongruous or coerced presentations, and even zero-effort impostor attempts. This unknown intention also causes false alarms by classifying some suspicious actions as potential presentation attacks, *e.g.*, non-conformant presentation due to illness, fatigue or presentation of artificial objects for cosmetic or health reasons. This complicates the classification of attacks and stimulates on-going scientific discussion in the field of how to efficiently deal with presentation attack detection (abbreviated further as PAD).

In this work we focus on iris liveness detection, *i.e.*, identification of liveness symptoms that could prove the authenticity of the eye and the willingness of the subject to be registered by the sensor. Instead of more commonly used static properties of the eye or its tissue, we use dynamics of the pupil registered under visible light stimuli. Since the pupil reacts involuntarily when the light intensity changes, it is difficult to conceal this phenomenon. As will be shown in the paper, the pupil dynamics are not trivial, making it difficult to mimic them for artificial objects. In our tests we decided not to use static objects such as iris paper printouts or patterned contact lenses, since in such cases we would be assured of success (static objects do not present significant dynamics, apart from some measurement noise, and thus are easily recognizable when dynamics is the key). Instead, to assess the proposed method performance, we classify spontaneous pupil oscillations (often called *hippus*) and normal pupil reactions to a positive surge of visible light, thus making the tests more realistic. To our best knowledge, this is the only work that employs pupil dynamics for liveness detection and which is evaluated on dynamic, real objects rather than static artifacts.

The paper is organized as follow: Section II gives a brief summary of error metrics used in the paper. Section III quotes and categorizes the most important past work on PAD related to iris recognition. Section IV describes a database of eye movies collected for this research. In Section V we provide theoretical backgrounds of the data pre-processing and

Manuscript received June 29, 2014; revised November 9, 2014; accepted November 28, 2014. Date of publication February 2, 2015. The associate editor coordinating the review of this manuscript and approving it for publication was Prof. Arun Ross.

The author is with the Institute of Control and Computation Engineering, Warsaw University of Technology, ul. Nowowiejska 15/19, 00-665 Warsaw, Poland, and also with the Research and Academic Computer Network - research institute (NASK), ul. Wawozowa 18, 02-796 Warsaw, Poland (e-mail: aczajka@elka.pw.edu.pl).

Full citation: Adam Czajka, "Pupil Dynamics for Iris Liveness Detection", IEEE Transactions on Information Forensics and Security, Vol. 10, No, 4, pp. 726-735, April 2015; DOI: 10.1109/TIFS.2015.2398815

modeling of pupil dynamics. Section VI presents experimental results that are discussed in Section VII.

II. Error metrics used

False rejections and false acceptances are common errors in biometrics. These refer to mistakenly rejecting or accepting claimed identity. In theory, we could use the same nomenclature in the context of liveness detection by a simple change of the claim from 'identity' to 'liveness'. However, an international discussion in this field suggests distinguishing error estimators related to presentation attack detection from those describing the biometric recognition. We thus follow the very last ISO/IEC proposal [1] and describe system performance at the PAD level by the following estimators:

a) Attack Presentation Classification Error Rate (APCER): proportion of attack presentations that were incorrectly classified as authentic presentations.

b) Normal Presentation Classification Error Rate (NPCER): proportion of authentic presentations incorrectly classified as attacks.

Occasionally, we also need a specific system operating point, describing jointly the APCER and NPCER:

c) Equal Error Rate (EER): value of APCER and NPCER when they are equal (analogous to the recognition performance analysis which employs equality of false rejections and false acceptances in definition of EER).

III. Presentation attack detection in iris recognition: past work

A. First demonstrations of vulnerabilities

Fifteen years have passed since Daugman's first proposal on how the iris recognition system can be spoofed by the eye printout [2]. Three years later, this idea was proved due to the first security evaluation of commercial iris recognition systems by Thalheim *et al.* [3]. During these tests simple iris printouts with a hole cut in place of the pupil were used. This gimmick made it possible to stultify an iris detection method implemented in the tested device. Disjoint frequency ranges employed in the tested iris coding (low frequencies) and in the printing process (high frequencies) made the printing artifacts 'invisible' to the iris feature extraction processes. This allowed them to print, present and positively verify a given iris. Pioneer research by Thalheim *et al.* stimulated others presenting their own security evaluation of additional, previously untested hardware, and again showing alarming lack of effective countermeasures in the commercial equipment [4], [5].

B. Scientific papers

From these first findings we observe a constant full bloom of PAD methods, characterized by a different sophistication level and kind of signals that may be analyzed when observing the eye. To summarize the current state of the art, we introduce four categories of the PAD methods characterized by way of measurement and dynamics of the observed object: passive or active measurement of a static or dynamic object. In the next paragraphs we provide the most prominent research results for each category.

Passive measurement of a static object. Methods of this kind employ a still image able to reveal only static eye features. No additional active measurement steps are performed. Usually the same picture as used in the recognition is employed for liveness detection. These approaches are still very attractive because no additional investment is made in iris capture hardware, even at the cost of limited reliability. The pioneer idea comes from Daugman [2], who noticed that the amplitude spectrum of the printed irides contains fake patterns, as opposed to smooth spectra obtained for authentic eyes. The first proposal on how to automatically find these 'fake frequencies' within the amplitude spectrum was probably made by Pacut and Czajka [5], and involved follow-up investigations [6], [7] that finally reported correct recognition of more than 95% of iris printouts (when no false rejections of alive samples were encountered).

Wei *et al.* [8] are probably the first authors to analyze three iris image properties to detect a patterned contact lens: image sharpness, Gabor-based filtering and second-order iris region statistics. The authors report good performance for the latter two approaches (98.3% and 100% of correct recognition rate, correspondingly), although admitting their high dependency on the printed contact lens pattern type. The small number (20) of artificial irides used should be taken into account when generalizing these results. He *et al.* [9] use wavelet packets analysis to calculate the liveness features classified by SVM (Support Vector Machine) with radial basis kernel. The authors report correct recognition of iris paper printouts even if intentionally blurred due to motion. He *et al.* [10] employ AdaBoost learning to select the best LBP-based (Local Binary Patterns) liveness features and Gaussian kernel density estimation is used to generalize the AdaBoost classifier. The authors report 99.33% correct recognition of fakes at the alive rejection rate of 2.64%, calculated for the evaluation database gathering 300 images of 20 different kinds of contact lenses, a few printouts and glassy eyes. Zhang *et al.* [11] use SVM to classify authentic iris images and patterned contact lens within the LBP feature space. Authors report CCR=99.14% (correct classification rate) calculated for 55 different types of contacts worn by 72 subjects and averaged through four different capture devices. This promising CCR drops to 88.05% in cross-validation scenario (training and testing performed on samples captured by different cameras).

Those promising, yet single image, properties were later used jointly to form multidimensional, image quality-based liveness indicators. Galbally *et al.* [12] apply feature selection methodology to find the best combination of liveness features among 22 proposed simple iris geometrical or frequency descriptors. Although they report perfect recognition of printouts and alive eyes, this may be specific to the low quality of printouts applied, as this result was based solely on segmentation outcomes (information on occlusions fused with pupil-to-iris radii ratio). We should rather expect the fake samples to result in correct segmentation, if they are used in real attacks. Nevertheless, the idea of merging different quality covariates

has high potential and it was applied later by Galbally *et al.* [13] along with quadratic discriminant analysis to detect 99.75% of iris printouts, simultaneously falsely rejecting 4.2% of the authentic eyes. They selected 25 quality measures that are complementary in detecting different attack types and that could be calculated efficiently in real time. This approach was also able to detect 99.2% synthetic irides at NPCER=3.4%.

Active measurement of static object. Methods of this kind realize the active measurement (besides the normal process of iris recognition) revealing some structural properties of the eye, yet not using eye dynamics. A typical example is detection of Purkinje reflections, *i.e.*, specular spots generated by illumination at inner and outer boundaries of the cornea and the eye lens. The idea originally proposed by Daugman [2] had been elaborated later by Lee *et al.* [14], who use two collimated NIR light sources (additional to the illuminants used for iris recognition) to generate and measure the Purkinje spots. Experiments done for eye images of 30 persons (including 10 wearing glasses and 10 wearing contact lens), 10 samples of paper printouts, 2 samples of printed contact lens, and 2 samples of 3D eye models lead to promising EER=0.33%. One should note that detection of Purkinje reflections requires high image sharpness, far better than normally required by iris recognition methods.

Connell *et al.* [15] use the fact that the authentic iris (in low resolution) is roughly flat, in contrary to a printed contact lens that reveals a convex shape. Hence, the authors use a structured light (popular in 3D facial imaging) generated by a miniature projector to capture the three-dimensional properties of the anterior part of the eyeball. This approach tested for images captured for only one subject and six different contact lenses presented perfect recognition of fakes.

When zooming in on the iris to see its muscle fibers, we end up with a structure that is no longer flat. When observed in higher resolution the trabeculae generate shadows when illuminated by light from different directions. Such shadows should not be present when smooth imitations (like paper printouts) are observed, hence some researchers use this method to distinguish flat artifacts from ragged, alive iris muscle. The first approach known to us on how to utilize the three dimensionality of the iris to determine its authenticity comes from Lee *et al.* [16]. The authors used wavelet decomposition to find 3D liveness features classified by SVM. Reported EER=0.33% was achieved for 600 live samples collected for 60 volunteers (some of them wearing glasses or contact lens) and for 600 fake samples prepared for different artifact types (printouts, photographs, printouts with contact lens, artificial images made from silicon or acrylic, and patterned contact lens). Hughes *et al.* [17] noticed that wearing patterned contact lens makes the observed iris pattern more convex (*i.e.*, lying on the lens surface), in contrast with the unobstructed, authentic iris, whose pattern lies roughly on a plane. Hence, they transformed a liveness detection problem into a problem of classifying the surface shape observed within the iris region. The authors captured stereo images of the iris in visible light for 4 persons, and additionally asked two of those four volunteers to wear contact lens (transparent and patterned) when capturing the images. They report perfect recognition of irides not equipped with contact lenses (or when transparent lenses are worn) from those wearing patterned contacts.

Park *et al.* [18] propose an interesting solution by using a few multi-spectral iris images instead of a typically applied single image taken in near infrared. The authors used a specialized tunable crystal filter offering very selective (10 nm band) illumination starting from 650 nm up to 1100 nm. The image used in recognition results in a gradient-based image fusion and presents no iris structure if the image is a printout, unlike authentic images providing useful iris features. The authors claim perfect performance, yet tests are shown for 4 different eyes only. Lee *et al.* [19] also use differences in multi-spectral light absorption by the eye tissues. The authors first calculate the ratio of iris-to-sclera image intensity (in pre-selected iris and sclera small regions). Since both the iris and the sclera have different light absorption properties depending on the wavelength of the illuminating light, this ratio differs when the light wavelength changes. Indeed, one may judge the authenticity of the sample by calculating the quotient of these ratios for two different illuminant wavelengths (750 nm and 850 nm are used in the paper). The authors demonstrate zero APCER and a small NPCER=0.28% for 2800 authentic iris images, 400 images of paper printouts and 30 images of plastic eyes. Not surprisingly however, this method falsely accepts 40% of colored contact lenses due to their transparency to the multi-spectral light applied in this work.

Passive measurement of dynamic object. In this group we detect dynamic properties of the measured object, yet without its stimulation. A natural example is detection of *hippus*, *i.e.*, spontaneous pupil size oscillations [2]. Although the idea of using hippus for liveness detection has existed for years and is often cited in papers, it is difficult to find reliable implementations to date. Additionally Pacut *et al.* suggest (after observing their own measurements) that the visibility of hippus is subject to the individual, and hence its reliability may be limited when applied to larger populations. A successful deployment of the hippus is shown by Fabiola *et al.* [20], however in the context of user authentication and not in liveness detection. EER=0.23% achieved by the authors when analyzing hippus in 50 persons suggests that the spontaneous movements of the pupil may deliver individual features. When added to the iris biometric template, they could serve as liveness indicators. The paper, however, does not include any tests with fake eyes to prove this hypothesis. If the iris image contains also the eyelids, one may adapt a spontaneous eye blinking detection, popular in face recognition and face liveness detection. Reported accuracy of blinks recognition is high (98% claimed by Cohn *et al.* [21] for 10 volunteers, or 88.8% for 20 subjects reported by Pan *et al.* [22]). One should note, however, that spontaneous blinks happen every few seconds; they are irregular and their frequency is subject dependent. Hence, when iris capture time plays an important role, detection of stimulated blinks (instead of spontaneous) seems to be a more adequate approach.

Active measurement of dynamic object. The last group of methods comprises those stimulating the object and analyzing its dynamics. The human eye delivers at least two types of dynamic features: those related to the entire eyeball and those

describing stimulated changes in pupil size. Komogortsev *et al.* observe the eye's horizontal saccade trajectories to differentiate authentic eyeballs and simulated behavior of mechanical replicas. The stimulus is a jumping point that had to be followed by 32 volunteers participating in the experiment. The smallest EER=5% is achieved when the eye movement model is unknown to the attacker, and EER=20% is declared by the authors when the occulomotor plant characteristics are available to imitate the eye's saccade. Some researchers employ the iris muscle deformations under changing illumination, like Kanematsu *et al.* [23] who calculate the iris image brightness variations after the light stimuli in the predefined iris regions. They report perfect recognition of alive irides and a few paper printouts. Puhan *et al.* [24] calculate the differences in iris texture for dilated and constricted irides, claiming that these differences should be large for an authentic eye and small for a printed contact lens. This claim, although correct in principle, has no proof of concept in the paper since the authors show results for two authentic eyes only and not for artifacts.

Scientific literature often mentions an attack with the use of LCD panels as the candidate for successful mimicking of eye dynamics, although no successful realization of this forgery is known so far. The iris acquisition equipment illuminates the eye by near infrared light (typical operating wavelength starts at 700 nm and ends at 900, as recommended by ISO/IEC 29794-6) and implements optical filters to cut the light outside this range. On the other hand, the LCD displays aim at presenting the contents to the user, and hence must operate in visible light (with wavelength not exceeding 700 nm). This causes the iris recognition cameras to be 'blind' to what is displayed by the LCD. Therefore this popular attack idea is impractical with off-the-shelf LCD displays. We do not know any LCD operating in near infrared light that could be used to play an eye movie.

One should note that no pupil dynamics are calculated in the above studies. Although the obvious idea to use pupil dynamic features for liveness detection has existed for years, there is only a small amount of research presenting proof of this concept along with adequate experimental results. Pacut *et al.* [5] used a dynamic pupil reaction model and neural classifier to perfectly recognize the authentic eyes and the iris printouts based on an image sequence database collected for 29 volunteers and more than 500 paper artifacts. At the same time, the authors applied for a patent in Poland [25], which was later extended to the USA [26]. Since they used the iris printouts in the research, which can be recognized by easier approaches, the potential of the method was neither appreciated nor presented. Czajka extended this study to show how this method recognizes the odd (or no) reactions of the eye [27], and this paper gives a thorough description of these findings.

C. Supporting activities

Besides the scientific endeavors, it is worth noting some other initiatives related to iris liveness detection. Clarkson University (USA), University of Notre Dame (USA), and Warsaw University of Technology (Poland) organized the first international iris liveness competition in 2013 [28]. This competition was a follow-up to three earlier liveness competitions, all devoted to fingerprint biometrics. The competition used paper iris printouts (815 images in total) and printed contact lenses (2240 images in total). Approximately 62% of contact lens images and 25% of paper printout images have been offered to participants as a training set, and the remaining data were used in evaluation of the delivered methods. Three universities decided to send their algorithms. Competition results demonstrate some interesting phenomena. First, it is clear that patterned contact lenses are much harder to detect when compared to recognition of paper printouts (0.65% of paper printout acceptance vs. 9.32% on average of printed contact lens acceptance achieved for the winning method). Second, the competition results show a clear dissonance between laboratory results presented by most of the scientific papers (typically showing perfect, or almost perfect recognition of fakes and alive samples) and third-party evaluation reporting average classification errors at a 10% level for a winning solution. These findings reinforce the importance of independent evaluations.

One may be also interested in TABULA RASA [29], a European project that is solely devoted to liveness detection. Some of the impressive project outcomes are devoted to iris recognition, *e.g.*, already cited deployment of iris image quality features in artifacts detection [12]. Biometrics Institute is an initiator of the Biometric Vulnerability Assessment Expert Group [30], an international group of experts that aims at raising the awareness about the importance of biometric vulnerability assessments and exchanging subject-related experiences. ISO/IEC JTC sub-committee No. 37 (Biometrics) is also about to issue a separate international standard devoted in full to presentation attack detection. These examples show that liveness detection in biometrics is not a fully solved issue or the results obtained to date do not satisfy both science and industry.

IV. Database of iris movies

A. Collection stand

To our best knowledge, there are no public collections of iris movies that would allow for this study of pupil dynamics. We decided to build suitable measuring equipment and gather our own set of *eye movies* captured in near infrared light. The core of the collection stand is the IrisCUBE camera [31] embedding The Imaging Source DMK 4002-IR b/w camera equipped with a SONY ICX249AL 1/2" CCD interline sensor of increased infrared sensitivity. The scene was illuminated by two near infrared illuminants ($\lambda = 850$ nm) placed horizontally and equidistantly to the lens. Our equipment applies a near infrared filter to cut any light with a wavelength lower than 800 nm. The IrisCUBE camera can capture 25 iris images per second, and the image quality significantly exceeds minimal ISO/IEC 19794-6 and ISO/IEC 29794-6 recommendations related to those aspects that are independent of the imaged subject. Since we wanted to guarantee repeatable capture conditions in the entire experiment, we enclosed the camera in a large, shaded box with a place where the subject positions his or her eyes

for acquisition of the image. We used visible LEDs, embedded into the frontal part of the camera case to help the user in positioning the head, as a visible light stimulus. This configuration guarantees the fixed position of the subject's head in each attempt and a stable distance between the subject's head and the camera (approximately 30 cm). It allows us to measure the pupil's reaction in complete darkness (regardless of external lighting conditions) as well as during the visible light step stimulation. However, one should be aware that pupil reaction may be less distinct when the eye is observed under bright ambient light (due to higher pupil constriction before the stimuli is applied).

B. Database statistics

We collected images for 52 distinct irides of 26 subjects. For 50 irides we captured 4 movies, and only 2 movies for a single person, making for 204 eye movies in total. Each movie lasts 30 seconds and presents spontaneous oscillations of the pupil size (first 15 seconds) and reaction to a step increase of light intensity (next 5 seconds), as well as the reaction to a negative step change in the illumination (last ten seconds). Since we capture 25 frames per second, the database volume sums up to $204 \times 30 \times 25 = 153\,000$ iris images illustrating pupil dilation and constriction processes. Figure 1 presents example frames and illustrates the moments of visible LED set-on and set-off.

C. Representation of actual and odd pupil reactions

In all research devoted to presentation attack detection we have a common difficulty in finding the classification function that divides our liveness feature space into two subspaces: authentic and fake. Since we typically build these classifiers by some learning procedures, we need samples representing those classes. This, unfortunately, leads us to methods that are specific to some kinds of fake objects. Generalization is almost impossible since we cannot predict the fantasy of the counterfeiters. In particular, past work summarized in Sec. III is devoted to detection of static artifacts, typically iris printouts, contact lenses or eye prosthetic models. Prior application of pupil dynamics for presentation attack detection [5], [26], demonstrating perfect performance, was also evaluated for paper printouts, but in such cases we should expect perfect performance, since static objects demonstrate no dynamics.

In this work we go beyond this limitation and develop the method that may recognize correct pupil dynamics and reject any behavior that mimics real pupil movements, or presents some odd, unexpected oscillations. In this research we decided to analyze the alive eyes only and to treat the spontaneous oscillations of the pupil as odd reactions to hypothetical (nonexistent in this case) light stimuli. This approach perfectly corresponds to what we understand under the 'liveness' term, namely the detection of vital symptoms of the analyzed object. Only an alive and authentic eye should demonstrate correct dynamics specific to a human organ. If after a sudden visible light impulse we observe nothing but hippus, this may denote that we observe a non-living eye. To organize our data according to our assumptions, we consequently crop two five-second sub-movies from each eye movie in the database. The first cropped sub-movie, representing odd eye reaction, starts when the measurement takes off, and ends after the fifth second of the measurement. The second sub-movie starts in the sixteenth second (exactly when the eye is stimulated by a visible light) and finishes in the twentieth second (exactly when the visible light is set off), see Fig. 1. This results in 204 movies lasting 5 seconds and representing odd reactions, and 204 movies representing expected pupil dynamics, also 5 seconds long.

We should be aware that the spontaneous oscillations of the pupil observed in complete darkness, or in a very bright ambient light, may have lower amplitude when compared to oscillations captured under a regular ambient light. The latter case allows the pupil to constrict and dilate with no distinct limitations, while complete darkness or a very bright ambient light causes the pupil to be already excessively constricted or dilated, hence allowing for only a limited change in its size.

V. Recognition of pupil dynamics

A. Data pre-processing

1) Pupil detection, segmentation and calculation of its size: Pupil dynamics is expressed by changes of its size. The *pupil size* is however an imprecise and general dimension that may be calculated in various ways. In this work we decided to use the most common, circular approximation of its – possibly irregular – shape. This is done intentionally due to three factors: a) high speed of circular segmentation, b) commonness of circular modeling in already deployed iris recognition methods, and c) unimportance of non circular deviations when describing the dynamics.

Having no ground truth related to iris location, we detect and localize the pupil in each frame independently. While *detection* refers to a statement of whether the pupil exists within the frame, the *localization* delivers its position. To localize a boundary between the pupil and the iris, we applied a Hough transform operating on *directional image* (estimation of an image gradient delivering both a gradient value and its direction). We parametrized the transform to make it sensitive to dark circular shapes and almost unresponsive to other dark shapes and light circles, such as specular reflections. Use of gradient and sensitivity to circular shapes makes this method surprisingly robust even if the pupil is 50% covered by eyelids. Consequently each eye movie is transformed into a time series of pupil radii, Fig. 1. We do not use gradient values that do not exceed a minimum threshold (set experimentally to the hardware setup that we employed). If there is no single gradient value exceeding the threshold, the method reports that no pupil could be detected. The latter realizes pupil detection, and helps to identify time moments when the eye is completely covered by eyelids.

2) Artifacts removal: Raw sequences of pupil radii are not perfect due to segmentation inaccuracy. In general, we encounter two kinds of disruptions: a) pupil detection errors (typically due to blinks fully covering the eye), and b) pupil segmentation noise (typically due to blinks in which the pupil is partially covered, eye motion, off-axis gaze, highly non-circular pupil shape that results in small oscillations of the

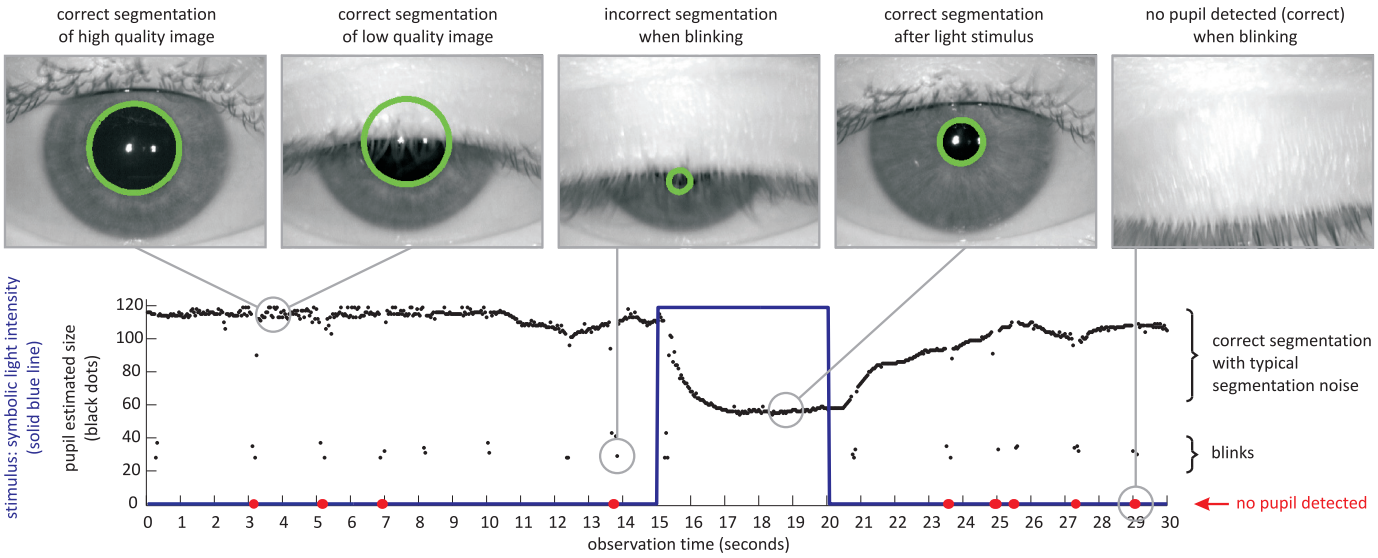

Fig. 1. Pupil size (black dots) measured automatically during a single experiment under the light stimuli (blue solid line). Note that capture of a real object results in a non-ideal sequence of pupil size due to blinks (black dots departing from the expected sequence), eye closure (red dots of zero ordinate denoting that no pupil is detected), or fluctuations of the segmentation process (revealing as a 'noise' in the sequence). Illustrating exemplars are shown at the top and linked to the corresponding moments of the sequence.

estimated pupil size, or simply algorithm mistakes). Errors of the first kind are identified by the pupil detection process. Those erroneous points can be easily omitted when modeling the pupil dynamics (marked as red dots lying on the horizontal axis in Fig. 1). However, the segmentation errors can be identified only to some extent when the pupil radius diverges significantly when compared to its neighboring values. These sudden collapses in pupil radius are mostly caused by partial blinks and – due to the speed of blink relative to 25 frames per second – they typically occupy several (or even isolated) values. We thus applied a median filtering with one second horizon (*i.e.*, 25 frames) applied as a sliding window.

B. Modeling of pupil dynamics

Light intensity surges generate obvious pupil constriction and dilation. Kohn and Clynes [32] noticed an asymmetry in pupil response depending on whether the flash is positive (from darkness to brightness) or negative, and proposed a reaction model that can be graphically envisioned as a two-channel transfer function of a complex argument s, Fig. 2.

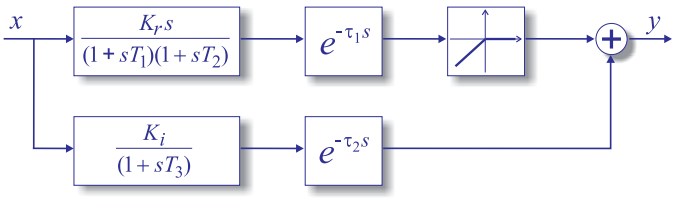

Fig. 2. Pupil dynamics model deployed in this work and derived from an original proposal of Kohn and Clynes [32]. Graph reprinted from [26].

The upper channel consists of a second order inertia with time constants T_1 and T_2, and a lag element characterized by τ_1. It models a transient behavior of the pupil only for positive light stimuli, what is guaranteed by a nonlinear function placed after the lag element and cutting down the channel response for negative stimuli. The channel gain is controlled by K_r. In turn, the lower channel is responsible for modeling long-term and persistent changes in pupil size, and answers by setting a new pupil radius after both the negative or positive light stimuli. It contains a first order inertia (with its speed controlled by T_3) and a lag element characterized by τ_2. The lower channel gain is controlled independently of the upper channel by K_i.

Calculating the inverse Laplace transform, we may easily obtain the model response $y(t;\phi)$ in time domain for a positive light stimuli at $t = 0$ as a sum of the upper and lower channel responses, $y_{\text{upper}}(t;\phi_1)$ and $y_{\text{lower}}(t;\phi_2)$, respectively:

$$y(t;\phi) = y_{\text{upper}}(t;\phi_1) + y_{\text{lower}}(t;\phi_2) \tag{1}$$

where

$$y_{\text{upper}}(t;\phi_1) = \begin{cases} -\frac{K_r}{T_1^2}(t-\tau_1)e^{-\frac{t-\tau_1}{T_1}} & \text{if } T_1 = T_2 \\ \frac{K_r}{T_2-T_1}\left(e^{-\frac{t-\tau_1}{T_1}} - e^{-\frac{t-\tau_1}{T_2}}\right) & \text{otherwise} \end{cases}$$

$$y_{\text{lower}}(t;\phi_2) = -K_i\left(1 - e^{-\frac{t-\tau_2}{T_3}}\right)$$

and

$$\phi = [\phi_1, \phi_2]^T = [K_r, T_1, T_2, \tau_1, K_i, T_3\tau_2]^T$$

are *liveness features*, *i.e.*, the vector of seven parameters setting the model response. Thus, the observed pupil dynamics (time series) is transformed to a single point in seven-dimensional, liveness feature space by solving the model fitting problem.

C. Searching for liveness features: fitting the model

Optimal model parameters $\widehat{\phi} = [K_r, T_1, T_2, \tau_1, K_i, T_3\tau_2]^T$ for each eye movie are identified by solving nonlinear least-squares curve fitting problem of the form:

$$\widehat{\phi} = \arg\min_{\phi\in\Phi} \sum_{i=1}^{N} (\widehat{y}(t;\phi) - y(t))^2 \tag{2}$$

where Φ is the set of possible values of ϕ, $y(t)$ is real (observed) change in the pupil size, $\widehat{y}(t;\phi)$ is the model response given the parameters ϕ and estimated for a given $y(t)$, and $t = 0, \ldots, t_{\max}$. We found that $t_{\max} \leq 1.5$ sec. makes this model useless; hence, in this work we analyze a multitude of optimization horizons starting from $t_{\max} = 1.6$ sec. and finishing with the maximum $t_{\max} = 5$ sec., Fig. 3.

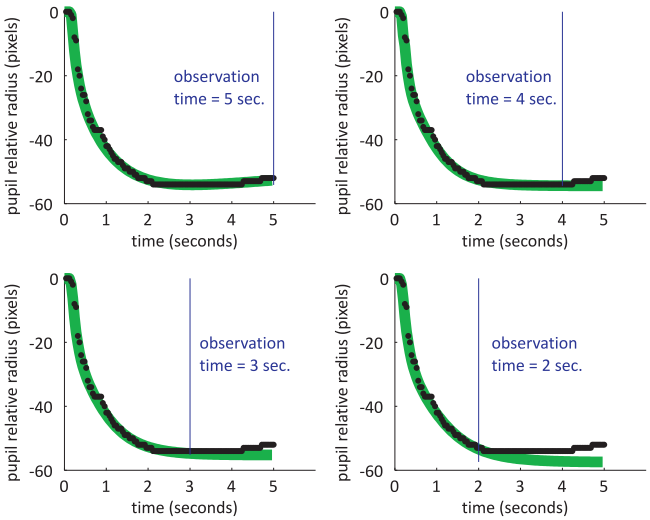

Fig. 3. Kohn and Clynes model responses (solid and thick green line) calculated for pre-processed measurement (black dots) shown in Fig. 1. In each case the modeling starts in $t = 0$. Top left graph presents the model output after 5 second observation, achieved for $\widehat{\phi} = [62.82, 0.10, 4.27, 0.17, 47.97, 0.84, 0.14]^T$. Remaining three graphs illustrate the degradation in modeling accuracy when the optimization horizon decreases.

D. Goodness of fit

To assess the goodness of fit we use normalized root mean square error, namely

$$\text{GoF} = \max\left(0, 1 - \frac{\|y(\cdot) - \widehat{y}(\cdot;\phi)\|}{\|y(\cdot) - \bar{y}(\cdot)\|}\right) \tag{3}$$

where $\bar{y}$ is the mean of y, and $\|\cdot\|$ indicates the 2-norm of a vector. GoF limits from 0, when $\widehat{y}$ is no better than a straight line fitting y, to 1 for a perfect fit.

E. Classification of the liveness features

Sample values of the liveness features shown in Fig. 4 suggest their heterogeneous discrimination power. However, we do not apply any feature selection method due to the low dimensionality of the feature space. Moreover, when identifying the model, we need to set all seven parameters.

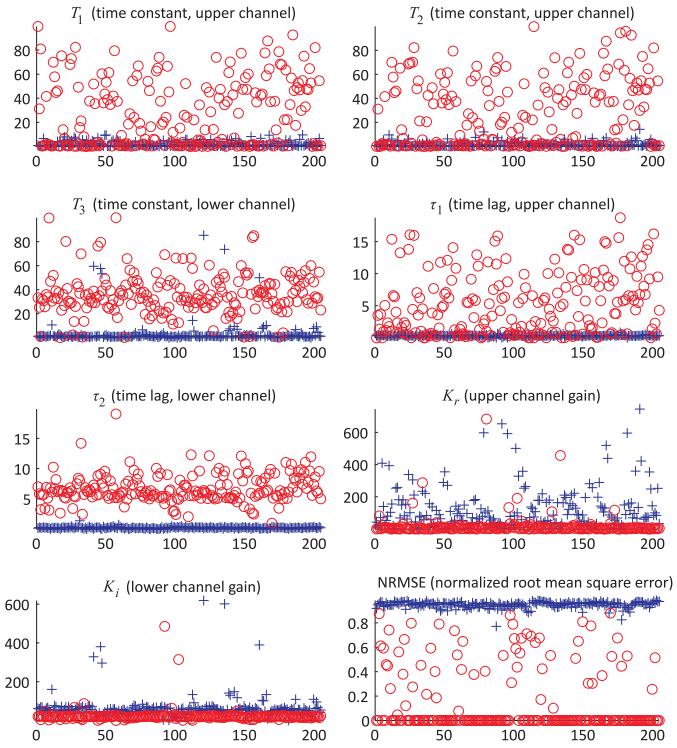

Fig. 4. Values of the liveness features $\widehat{\phi}$ calculated for the expected (blue crosses) and odd (red circles) pupil reactions for positive light stimulus and five second observation time. Results for all 204 eye movies are shown. Normalized root mean square error (NRMSE) is also shown in the bottom right graph, suggesting a far better fit for normal pupil reactions when compared to odd ones.

Therefore there is no practical rationale behind narrowing the feature set.

To build a classification function, we use the Support Vector Machine as one of the best off-the-shelf classifiers performing well in low dimensional feature spaces (as in our case). To approximate linear and nonlinear classification boundaries, we deployed linear SVM as well as radial basis function and polynomial kernels.

VI. Experiments and Results

A. Generating gallery and probe samples

In order to minimize the risk of underestimating the performance errors, we divide our dataset into two disjoint subsets used to train and evaluate a given method. The training subset is often called the *gallery*, while the subset used to evaluate the trained algorithm is called the *probe*. In ideal situation we have ample sizes of both gallery and probe subsets to provide statistical guarantees of the calculated errors that satisfy our needs. In a typical situation, however, the sizes of those sets are far below the ideal, and – depending on the original database size – different cross-validation techniques are used to answer how the specific results would generalize on the independent and unknown data. In biometrics we commonly use the k-fold and leave-n-out cross-validations, setting $k = 2$ in the former (two folds, possibly of equal size, corresponding to the gallery and probe subsets) and setting $n = 1$ in the latter (the gallery

consists of $n-1$ samples, while the remaining one sample forms a probe set).

In this work leave-one-out cross-validation is used, but leaving out *all* samples of a given person instead of using a single sample (*i.e.*, single time series). This scenario generates $n = 26$ runs of training-testing experiments (which is equal to the number of distinct subjects) instead of 204 (*i.e.*, number of all samples), but due to statistical dependency among samples of the same person, we believe in obtaining evaluation results unbiased by personal dependency.

B. Decision making

Relying solely on the classifier output is insufficient since some odd reactions of the eye may result in model parameters falling into the subspace representing authentic eye reactions. It is a good idea to analyze the goodness of fit simultaneously with the classifier output, as erroneously accepted samples may result from poor model identification. This builds a two-dimensional decision plane with classifier response on one axis and the goodness of fit on the other providing four decision regions, Fig. 5. We accept the observed object as alive only when the classifier decision is positive and the model fit is accurate.

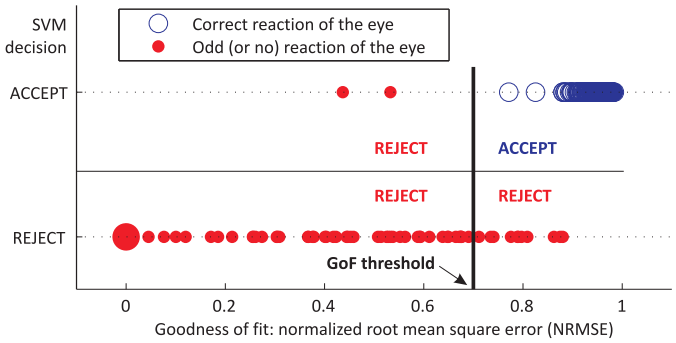

Fig. 5. Decision plane defined by the SVM output and the estimate of goodness of fit (GoF). This example shows that requiring some minimum value of GoF when calculating the liveness features improves the final decision: the method correctly rejected a few odd reactions mistakenly accepted by the SVM (represented by the red dots) but resulting from an inaccurate model (GoF below the threshold). This example is generated for all 204 samples classified by the linear SVM during 5 second observation period.

C. Assessment of the method performance

We had two objectives when performing the experiments: a) to assess the performance of the method and select the most reliable SVM kernel, and b) to find a minimum pupil observation time that is necessary to offer reasonable accuracy. The former answers the question of whether there is a theoretical potential in this approach. The latter estimates the chances of practical deployments in a biometric system, since the expected iris capture times should be short (not exceeding a few seconds).

Application of a leave-one-out procedure (leaving out all the samples for a given person) leads us to $n = 26$ estimation-evaluation experiments. That is, in each experiment we train three different SVMs (linear, polynomial and radial basis), along with eventual parameter optimization (in particular: order of polynomial kernel and attenuation parameter for radial basis kernel) using all samples for $n-1$ subjects. We then evaluate these SVMs on the unknown samples of the remaining subject. In each estimation experiment, we also set the goodness of fit threshold for later use in evaluating the classifier with the remaining samples. We decided to set the GoF threshold so as not to increase false rejections due to liveness detection, *i.e.*, we minimized NPCER. There is an important rationale behind this approach rather than minimizing the false acceptances of non-living eyes that comes both from theory and practice. Theoretical deliberations suggest that predicting the nature of – and hence resulting statistics related to – all the possible attacks is impossible. On the other hand, it is easier to develop statistical models for authentic biometric samples. Thus, it is reasonable to focus on authentic data when approximating a classification function and to accept that this classifier may generate some errors for fakes. This approach is more robust than an opposite approach in which we would fix the classification function tightly around specific fake samples, since the generality for other kinds of fakes would be weak and would decrease accuracy for authentic samples. This corresponds to practice, since the system developers are more resistant to the increased probability of false rejection and they are more likely to a higher probability of accepting the fakes (which is very high with no liveness detection anyway, and which always decreases when even a weak PAD method is applied).

Consequently, we performed $n = 26$ independent evaluations. The average error rates are presented for each SVM and each observation time as the final results (see Figs. 6, 7 and 8). Results show a few interesting outcomes. First, all the classifiers managed to perfectly differentiate the odd and natural reactions of the pupil if we can allow for 5 second observation (NPCER=APCER=0 for all 26 evaluations). Second, it seems that we may shorten the observation time to less than 3 seconds, since all the SVMs perform well for time horizons slightly exceeding 2 seconds. Third, the performance of three different SVMs is similar suggesting that building a linear classifier would be an adequate solution to obtain acceptable performance for the proposed liveness features.

VII. Merits and Limitations: Discussion

The outcomes shown in the last section suggest that pupil dynamics may deliver interesting liveness features when observing the eye for a short time (relative to the typical acquisition time of a few seconds in iris recognition). Mimicking pupil dynamics is difficult, and concealing one's own pupil reaction is impossible due to its involuntary nature. The medical literature reports also that the pupil reaction may change under stress. Therefore, we may even formulate the hypothesis that this is one of few methods that could recognize the capture under coercion.

Implementation of the proposed approach may have an additional, positive side effect. It is known that the accuracy of iris recognition may be affected by inconsistencies in pupil

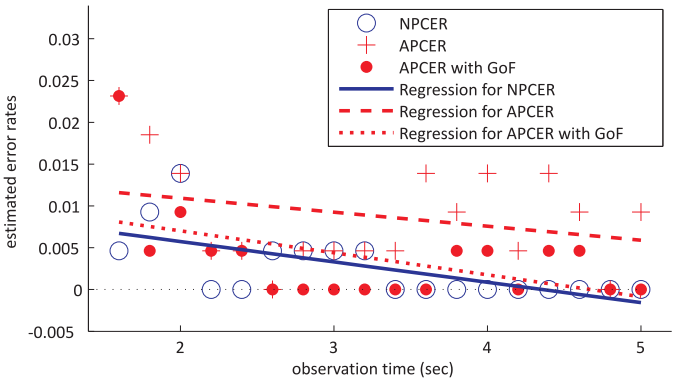

Fig. 6. Averaged error rates as a function of the observation time (calculations made every 200 ms starting from 1600 ms and ending after 5000 ms), achieved for **linear SVM**. Blue circles show the average (for 26 independent evaluations) proportion of authentic presentations incorrectly classified as attacks. Red crosses show averaged proportion of attack presentations that were incorrectly classified as authentic ones when we rely solely on the SVM output. Red dots suggest far better accuracy when the goodness of fit is analyzed along with the classification decisions. We added regression lines to illustrate linear trends as a function of the observation time.

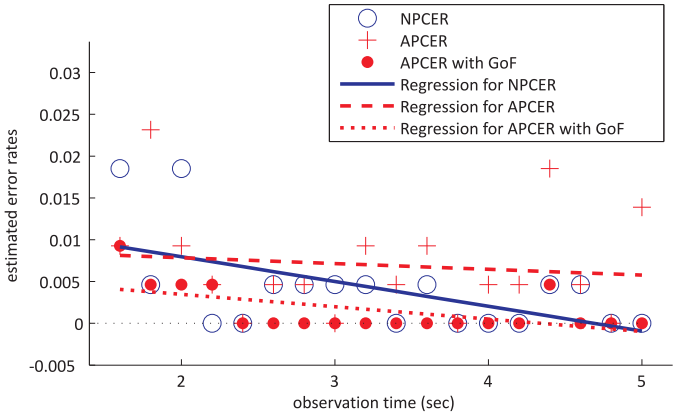

Fig. 7. Same as in Fig. 6, except the polynomial kernel is used in the SVM (with polynomial order equal to 3).

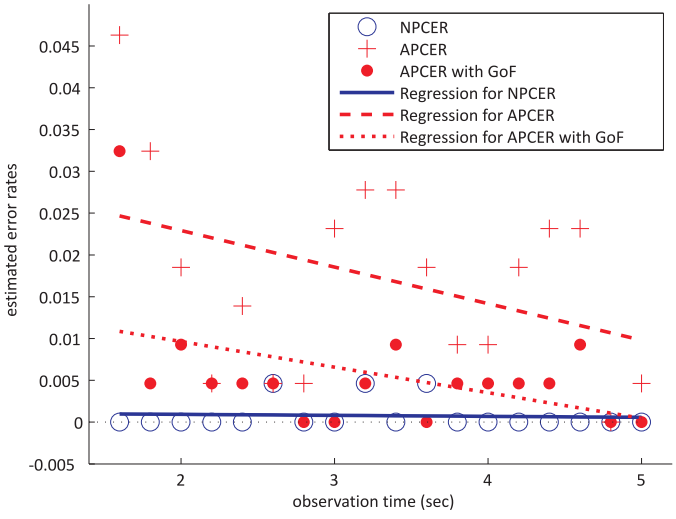

Fig. 8. Same as in Fig. 6, except that the radial basis kernel is used in the SVM.

size, especially when the pupil dilation differs significantly in the enrollment and authentication processes. The approach presented in this paper can paradoxically compensate for this phenomenon at no cost, in particular not introducing additional acquisition time. Namely, once the iris movie is captured, the biometric system can select one (or a few) iris images with different sizes of the pupil to perform the biometric recognition (no additional capture is needed). If the same system records the pupil size observed at the enrollment along with the reference template, it can select the frame with similar pupil size at the authentication stage. If there are no pupil size data connected to the reference template, the system can deploy multiple authentication images presenting different pupil sizes and select the lowest distance between the template and the authentication sample. This should significantly lower within-class variance of the iris comparison score distribution.

To complete our conclusions, we should also analyze the darker side of the coin. First, the measurement of dynamic features takes time. Not all applications allow for additional two seconds when capturing the iris. Second, limitation may come from the variability of dynamic features across different populations and more subtle changes in pupil size for elderly people. Since the database used in this study does not contain any measurement from elderly people, reported errors may be underestimated in their case. The third limitation may refer to the possible non-stationarity of pupil dynamics as a consequence of ingestion of different substances (*e.g.*, drugs or alcohol), an altered psychological state (*e.g.*, stress, relaxation, drowsiness or mental load). We do not know of scientific results that would thoroughly discuss the influence of these factors on pupil dynamics, yet it is easy to imagine that they are not unimportant. Since this work presents research results for people who are not stressed and who have not ingested any substance that could modify pupil reaction, we cannot guarantee that pupil dynamics is unaltered in these abnormal circumstances. Lest we also forget the surrounding environment, since the starting pupil size (and thus the amplitude of the reaction) depends on the intensity of ambient light. This research used data collected in darkness before applying light stimuli.

To conclude, this method seems to be a good candidate for robust liveness detection and has a high potential for practical applications. Keeping in mind its limitations, one may obtain an interesting element of the PAD implementation that is sensitive to features not offered by methods detecting static artifacts.

ACKNOWLEDGMENTS

The author would like to thank Mr. Rafal Brize, who collected the database of iris images used in this work under his Master's degree project lead by this author. The author is cordially grateful to Prof. Andrzej Pacut of Warsaw University of Technology for valuable remarks that significantly contributed to this research. The application of Kohn and Clynes model was inspired by research of Mr. Marcin Chochowski, who used parameters of this model as individual features in biometric recognition. This author, together with Prof. Pacut

and Mr. Chochowski, has been granted a US patent No. 8,061,842 which partially covers the idea deployed in this work. Last but not least, the author heartily thanks Barbara Mangione for corrections of English grammar and word usage.

REFERENCES

[1] ISO/IEC JTC 1/SC 37 Text of Working Draft 30107-3, "Information Technology – Presentation Attack Detection – Part 3: Testing, reporting and classification of attacks," February 28, 2014.

[2] J. Daugman, "Countermeasures against subterfuge," in *Biometrics: Personal Identication in Networked Society*, Jain, Bolle, and Pankanti, Eds. Amsterdam: Kluwer, 1999, pp. 103–121.

[3] L. Thalheim, J. Krissler, and P.-M. Ziegler, "Biometric Access Protection Devices and their Programs Put to the Test," Available online in c't Magazine, No. 11/2002, p. 114.

[4] T. Matsumoto, "Artificial fingers and irises: Importance of vulnerability analysis," in *Proceedings of the Seventh International Biometrics Conference and Exhibition*, 2004.

[5] A. Pacut and A. Czajka, "Aliveness detection for iris biometrics," in *40th Annual IEEE International Carnahan Conference on Security Technology*, 2006, pp. 122–129.

[6] X. He, Y. Lu, and P. Shi, "A fake iris detection method based on fft and quality assessment," in *Pattern Recognition, 2008. CCPR '08. Chinese Conference on*, Oct 2008, pp. 1–4.

[7] A. Czajka, "Database of iris printouts and its application: Development of liveness detection method for iris recognition," in *Methods and Models in Automation and Robotics (MMAR), 2013 18th International Conference on*, Aug 2013, pp. 28–33.

[8] Z. Wei, X. Qiu, Z. Sun, and T. Tan, "Counterfeit iris detection based on texture analysis," in *Pattern Recognition, 2008. ICPR 2008. 19th International Conference on*, Dec 2008, pp. 1–4.

[9] X. He, Y. Lu, and P. Shi, "A new fake iris detection method," in *Advances in Biometrics*, ser. Lecture Notes in Computer Science, M. Tistarelli and M. Nixon, Eds. Springer Berlin Heidelberg, 2009, vol. 5558, pp. 1132–1139.

[10] Z. He, Z. Sun, T. Tan, and Z. Wei, "Efficient iris spoof detection via boosted local binary patterns," in *Advances in Biometrics*, ser. Lecture Notes in Computer Science, M. Tistarelli and M. Nixon, Eds. Springer Berlin Heidelberg, 2009, vol. 5558, pp. 1080–1090.

[11] H. Zhang, Z. Sun, and T. Tan, "Contact lens detection based on weighted lbp," in *Pattern Recognition (ICPR), 2010 20th International Conference on*, Aug 2010, pp. 4279–4282.

[12] J. Galbally, J. Ortiz-Lopez, J. Fierrez, and J. Ortega-Garcia, "Iris liveness detection based on quality related features," in *Biometrics (ICB), 2012 5th IAPR International Conference on*, March 2012, pp. 271–276.

[13] J. Galbally, S. Marcel, and J. Fierrez, "Image quality assessment for fake biometric detection: Application to iris, fingerprint, and face recognition," *Image Processing, IEEE Transactions on*, vol. 23, no. 2, pp. 710–724, Feb 2014.

[14] E. Lee, K. Park, and J. Kim, "Fake iris detection by using purkinje image," in *Advances in Biometrics*, ser. Lecture Notes in Computer Science, D. Zhang and A. Jain, Eds. Springer Berlin Heidelberg, 2005, vol. 3832, pp. 397–403.

[15] J. Connell, N. Ratha, J. G. Ruud, and Bolle, "Fake iris detection using structured light," in *Acoustics, Speech and Signal Processing (ICASSP), 2013 IEEE International Conference on*, May 2013, pp. 8692–8696.

[16] E. C. Lee and K. R. Park, "Fake iris detection based on 3D structure of iris pattern," *International Journal of Imaging Systems and Technology*, vol. 20, no. 2, pp. 162–166, 2010.

[17] K. Hughes and K. W. Bowyer, "Detection of contact-lens-based iris biometric spoofs using stereo imaging," in *System Sciences (HICSS), 2013 46th Hawaii International Conference on*, Jan 2013, pp. 1763–1772.

[18] J. Park and M. Kang, "Iris recognition against counterfeit attack using gradient based fusion of multi-spectral images," in *Advances in Biometric Person Authentication*, ser. Lecture Notes in Computer Science, S. Li, Z. Sun, T. Tan, S. Pankanti, G. Chollet, and D. Zhang, Eds. Springer Berlin Heidelberg, 2005, vol. 3781, pp. 150–156. [Online]. Available: http://dx.doi.org/10.1007/11569947_19

[19] S. J. Lee, K. R. Park, and J. Kim, "Robust fake iris detection based on variation of the reflectance ratio between the iris and the sclera," in *Biometric Consortium Conference, 2006 Biometrics Symposium: Special Session on Research at the*, September 2006, pp. 1–6.

[20] F. M. Villalobos-Castaldi and E. Suaste-Gómez, "A new spontaneous pupillary oscillation-based verification system," *Expert Syst. Appl.*, vol. 40, no. 13, pp. 5352–5362, 2013.

[21] J. Cohn, J. Xiao, T. Moriyama, Z. Ambadar, and T. Kanade, "Automatic recognition of eye blinking in spontaneously occurring behavior," *Behavior Research Methods, Instruments, and Computers*, vol. 35, no. 3, pp. 420–428, 2003.

[22] G. Pan, Z. Wu, and L. Sun, "Liveness detection for face recognition," in *Recent Advances in Face Recognition*, K. Delac, M. Grgic, and M. S. Bartlett, Eds. Springer Berlin Heidelberg, 2008, pp. 109–124.

[23] M. Kanematsu, H. Takano, and K. Nakamura, "Highly reliable liveness detection method for iris recognition," in *SICE, 2007 Annual Conference*, Sept 2007, pp. 361–364.

[24] N. Puhan, N. Sudha, and A. Suhas Hegde, "A new iris liveness detection method against contact lens spoofing," in *Consumer Electronics (ISCE), 2011 IEEE 15th International Symposium on*, June 2011, pp. 71–74.

[25] A. Czajka, A. Pacut, and M. Chochowski, "Sposob testowania zywotnosci oka i urzadzenie do testowania zywotnosci oka (method of eye aliveness testing and device for eye aliveness testing)," PL Patent Application P380 581, September 7, 2006.

[26] ——, "Method of eye aliveness testing and device for eye aliveness testing," US Patent 8 061 842, November 22, 2011. [Online]. Available: http://www.lens.org/images/patent/US/8061842/B2/US_8061842_B2.pdf

[27] A. Czajka, "Pupil dynamics for presentation attack detection in iris recognition," in *International Biometric Performance Conference (IBPC), NIST, Gaithersburg*, April 2014, pp. 1–3. [Online]. Available: http://biometrics.nist.gov/cs_links/ibpc2014/presentations/09_thursday_czajka_IBPC.2014.Adam.Czajka.pdf

[28] D. Yambay, J. Doyle, K. Bowyer, A. Czajka, and S. Schuckers, "LivDet-Iris 2013: Iris Liveness Detection Competition," in *Biometrics: Theory, Applications and Systems (BTAS), 2013 IEEE Sixth International Conference on*, September 29 – October 2 2013. [Online]. Available: http://people.clarkson.edu/projects/biosal/iris

[29] Trusted Biometrics under Spoofing Attacks (TABULA RASA). Project funded by the European Commission, under the Seventh Framework Programme. [Online]. Available: http://www.tabularasa-euproject.org

[30] Biometric Vulnerability Assessment Expert Group (BVAEG). [Online]. Available: http://www.biometricsinstitute.org/pages/biometric-vulnerability-assessment-expert-group-bvaeg.html

[31] A. Czajka and A. Pacut, "Iris Recognition System Based on Zak-Gabor Wavelet Packets," *Journal of Telecommunications and Information Technology*, no. 4, pp. 10–18, 2010.

[32] M. Kohn and M. Clynes, "Color dynamics of the pupil," *Annals of New York Academy of Science*, vol. 156, no. 2, pp. 931–950, 1969. Available online at Wiley Online Library (2006).

Adam Czajka Received his M.Sc. in Computer Control Systems in 2000 and Ph.D. in Biometrics in 2005 from Warsaw University of Technology (both with honors). Since 2003 he has been with Warsaw University of Technology, and since 2002 he has been with Research and Academic Computer Network (NASK). A. Czajka is Chair of the Biometrics and Machine Learning Laboratory at the Institute of Control and Computation Engineering and Head of the Postgraduate Studies on Security and Biometrics (2011-). He is V-ce Chair of the NASK Biometrics Laboratory and a member of the NASK Research Council (2006-). A. Czajka is Chair of the Technical Committee on Biometrics No. 309 (2014-) and a member of the Technical Committee No. 182 on Information Security in IT Systems (2007-) of Polish Normalization Committee (PKN). He is an expert of the ISO/IEC SC37 on Biometrics. Recently, Dr. Czajka has been Visiting Associate Professor at the University of Notre Dame, Indiana, USA (Fall 2014).